Dependent Randomization in Parallel Binary Decision Fusion

July 2, 2020

Weiqiang Dong and Moshe Kam
Department of Electrical and Computer Engineering
New Jersey Institute of Technology
Newark, New Jersey 07102
Email: wd35@njit.edu, kam@njit.edu

Supplement file, Part C

C-1 Proof: $P_d^{C'}$ is the maximum probability of detection when either (i) $A' \in \Omega^A$ or (ii) $B' \in \Omega^B$ or both ($A' \in \Omega^A$ and $B' \in \Omega^B$) (Section V-C)

C-2 An efficient way to find A' from Ω^A if $A' \in \Omega^A$ and B' from Ω^B if $B' \in \Omega^B$ (Section V-D)

In this file, the index of each Table/Figure/Equation has a prefix “C-”; the index of each Table/Figure/Equation that appears in the main paper has a prefix “P-”.

SUPPLEMENT FILE, PART C

When the DFC only synchronizes with the m LDs in Y, the system operates at some point on *ROC curve A* with probability p and some point on *ROC curve B* with probability $1-p$. *ROC curve A* can be drawn by connecting points in $\Omega^A = \{w_1^A = (0,0), w_2^A, \ldots, w_{mA-1}^A, w_{mA}^A = (1,1)\}$ sequentially and *ROC curve B* can be drawn by connecting points in $\Omega^B = \{w_1^B = (0,0), w_2^B, \ldots, w_{mB-1}^B, w_{mB}^B = (1,1)\}$ sequentially. We want to find a specific point on *ROC curve A*, denoted as A', and a specific point on *ROC curve B*, denoted as B' that allow the system to maximize the probability of detection while satisfying the probability of false alarm constraint. The optimal resulting system operating point $C' = (P_f^{C'}, P_d^{C'})$ is on the line segment connecting A' and B'.

Part C-1 proves a result used in Section V-C of the paper: $P_d^{C'}$, the probability of detection at the redesigned operating point, is the maximum probability of detection when either (i) $A' \in \Omega^A$ or (ii) $B' \in \Omega^B$ or both ($A' \in \Omega^A$ and $B' \in \Omega^B$).

Part C-2 provides an efficient way to locate A' if $A' \in \Omega^A$ and B' if $B' \in \Omega^B$ (per Section V-D of the paper).

C-1. Proof: $P_d^{C'}$ ((P-29) in the paper) is the maximum probability of detection when either (i) $A' \in \Omega^A$ or (ii) $B' \in \Omega^B$ or both ($A' \in \Omega^A$ and $B' \in \Omega^B$)

We are going to show that for $P_d^{C'}$ in (P-29) to be the maximum probability of detection either (i) $A' \in \Omega^A$ or (ii) $B' \in \Omega^B$ or both ($A' \in \Omega^A$ and $B' \in \Omega^B$).

Point $a = (P_f^a, P_d^a)$ is on *ROC curve A*, which is a concave linear ROC curve. P_d^a can be expressed as

$$P_d^a = f_A(P_f^a) P_f^a + b_A(P_f^a). \tag{C-1}$$

$f_A(P_f^a)$ and $b_A(P_f^a)$ are respectively the slope and the P_d-axis intercept of the line segment on *ROC curve A* that passes through point a. $f_A(P_f^a)$ is a decreasing piecewise-constant function of P_f^a and $b_A(P_f^a)$ is an increasing piecewise-constant function of P_f^a.

Similarly, point $b = (P_f^b, P_d^b)$ is on ***ROC curve B***, which is a concave linear ROC curve. P_d^b can be expressed as

$$P_d^b = f_B(P_f^b)P_f^b + b_B(P_f^b). \tag{C-2}$$

$f_B(P_f^b)$ and $b_B(P_f^b)$ are respectively the slope and the P_d-axis intercept of the line segment on *ROC curve B* that passes through point b. $f_B(P_f^b)$ is a decreasing piecewise-constant function of P_f^b and $b_B(P_f^b)$ is an increasing piecewise-constant function of P_f^b.

Figure C-1 shows the relation between $a = (P_f^a, P_d^a)$ (cyan circle) on *ROC curve A*, $b = (P_f^b, P_d^b)$ (purple triangle) on *ROC curve B*, and the resulting operating point $c = (P_f^c, P_d^c) = (pP_f^a + (1-p)P_f^b = \alpha, pP_d^a + (1-p)P_d^b)$ (purple square), calculated by (P-26) and (P-27), which is the intersection of $P_f = \alpha$ and line ab.

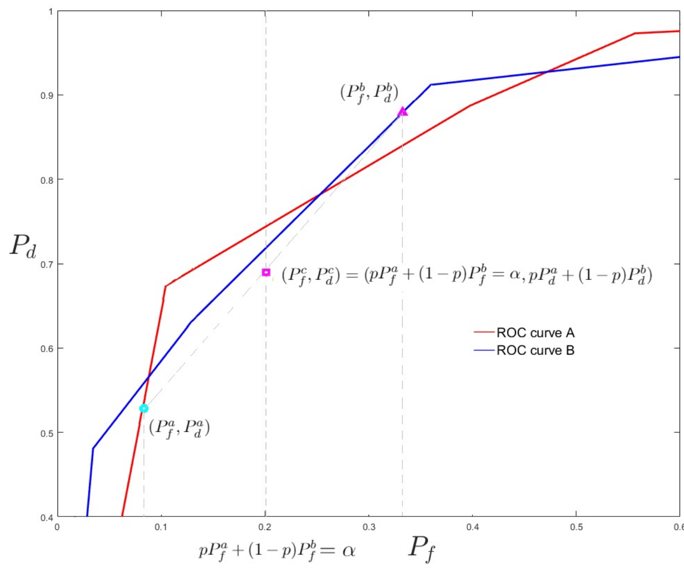

Figure C-1: The system operates at $a = (P_f^a, P_d^a)$ (cyan circle) with probability p. The system operates at $b = (P_f^b, P_d^b)$ (purple triangle) with probability $1-p$. The resulting operating point is $c = (P_f^c, P_d^c) = (pP_f^a + (1-p)P_f^b = \alpha, pP_d^a + (1-p)P_d^b)$, shown by the purple square.

From (P-26), when the probability of false alarm constraint is met, P_f^a is a decreasing function of P_f^b (and P_f^b is a decreasing function of P_f^a):

$$P_f^a = \frac{\alpha - (1-p)P_f^b}{p}, \text{ and,} \tag{C-3}$$

$$P_f^b = \frac{\alpha - pP_f^a}{1-p}. \tag{C-4}$$

Combining (P-27), (C-1), and (C-2), we have:

$$\begin{aligned} P_d^c &\overset{\text{from } (P-27)}{=} pP_d^a + (1-p)P_d^b \\ &\overset{\text{from } (C-1),(C-2)}{=} p(f_A(P_f^a)P_f^a + b_A(P_f^a)) + (1-p)(f_B(P_f^b)P_f^b + b_B(P_f^b)). \end{aligned} \tag{C-5}$$

From (C-4), P_f^b is a decreasing function of P_f^a (from (C-3), P_f^a is also a decreasing function of

P_f^b). Substitute (C-4) into (C-5), P_d^c can be expressed as a function of P_f^a [3]:

$$\begin{aligned} P_d^c &= \boldsymbol{s}P_f^a + \boldsymbol{l}, \text{where} \\ \boldsymbol{s} &= p[f_A(P_f^a) - f_B(P_f^b)], \\ &\overset{\text{from }(C-4)}{=} p[f_A(P_f^a) - f_B(\frac{\alpha - pP_f^a}{1-p})], \text{and} \\ \boldsymbol{l} &= f_B(P_f^b)\alpha + pb_A(P_f^a) + (1-p)b_B(\frac{\alpha - pP_f^a}{1-p}) \end{aligned} \tag{C-6}$$

which have the following properties:

Property 1:*P_d^c is a continuous function of P_f^a.*

P_d^a is a continuous function of P_f^a and P_d^b is a continuous function of P_f^b (since a and b are points on continuous ROC curves). Meanwhile, since P_f^b is a continuous function of P_f^a (from (C-4)), P_d^b is a continuous function of P_f^a. P_d^c is a weighted sum of P_d^a and P_d^b (from P-27), therefore it is a continuous function of P_f^a.

Property 2: *P_d^c is a piecewise-linear function of P_f^a.*

Since both *ROC curve A* and *ROC curve B* are composed of finite line segments, in (C-6), $f_A(P_f^a), f_B(\frac{\alpha-pP_f^a}{1-p}), b_A(P_f^a),$ and $b_B(\frac{\alpha-pP_f^a}{1-p})$ are piecewise-constant functions of P_f^a. Therefore, P_d^c is a piecewise-linear function of P_f^a. The graph of P_d^c consists of finite number of line segments on the $P_f^a - P_d^c$ plane. The slope of each line segment is $s = f_A(P_f^a) - f_B(\frac{\alpha-pP_f^a}{1-p})$ and the P_d^c-axis intercept of each line segment is $l = f_B(P_f^b)\alpha + pb_A(P_f^a) + (1-p)b_B(\frac{\alpha-pP_f^a}{1-p})$.

Property 3: *P_d^c is a concave function of P_f^a.*

From properties 1 and 2, P_d^c is a continuous piecewise-linear function of P_f^a. The slope of each line segment is $s = f_A(P_f^a) - f_B(P_f^b)$. $f_A(P_f^a)$ is a decreasing function of P_f^a since *ROC curve A* is piecewise-linear concave. $f_B(P_f^b) = f_B(\frac{\alpha-pP_f^a}{1-p})$ is an increasing function of P_f^a since $f_B(P_f^b)$ is a decreasing function of P_f^b and P_f^b is a decreasing function of P_f^a. In (C-6), $s = f_A(P_f^a) - f_B(P_f^b)$

[3]Similarly, if we substitute (C-3) into (C-5), then P_d^c can be expressed as a function of P_f^b.

is a decreasing function of P_f^a. In this circumstance, P_d^c is a concave function of P_f^a.

Property 4: The range of P_f^a is $P_f^a \in [max(0, \frac{\alpha+p-1}{p}), min(1, \frac{\alpha}{p})]$ when the probability of false alarm constraint is satisfied.

Since points a and b are on ROC curves, we have $P_f^a \in [0,1]$ and $P_f^b \in [0,1]$. From (C-4), when the probability of false alarm constraint is satisfied, $P_f^b = 0$ indicates $P_f^a = \frac{\alpha}{p}$ and $P_f^b = 1$ indicates $P_f^a = \frac{\alpha+p-1}{p}$. Therefore, $P_f^b \in [0,1]$ indicates that $P_f^a \in [\frac{\alpha+p-1}{p}, \frac{\alpha}{p}]$. Therefore, the range of P_f^a is $P_f^a \in [max(0, \frac{\alpha+p-1}{p}), min(1, \frac{\alpha}{p})]$.

From Properties 1-4, P_d^c is a piecewise-linear concave function of P_f^a and its domain satisfies $P_f^a \in [max(0, \frac{\alpha+p-1}{p}), min(1, \frac{\alpha}{p})]$. Note that a piecewise-linear concave function sometimes can be a monotonic linear function. We discuss three different cases about finding the maximum of P_d^c: (1) P_d^c is a non-decreasing linear function of P_f^a; (2) P_d^c is a non-increasing linear function of P_f^a; (3) P_d^c is first non-decreasing function and then a non-increasing function of P_f^a. Figure C-2 shows a graphical illustration of these three cases.

Case (1): $s \geq 0$ when $P_f^a = max(0, \frac{\alpha+p-1}{p})$ and when $P_f^a = min(1, \frac{\alpha}{p})$. In this case, P_d^c is a non-decreasing function of P_f^a and the maximum value of P_d^c is achieved at $P_f^a = min(1, \frac{\alpha}{p})$. If $P_f^a = min(1, \frac{\alpha}{p}) = 1$, since point $a = (P_f^a, P_d^a)$ is on *ROC curve A*, when $P_f^a = 1$, $P_d^a = 1$. Therefore, $A' = (1,1) = \omega_{mA}^A \in \Omega^A$. If $P_f^a = min(1, \frac{\alpha}{p}) = \frac{\alpha}{p} = \frac{\alpha-(1-p)0}{p} = \frac{\alpha-(1-p)P_f^{\omega_1^B}}{p} \overset{\text{from }(C-3)}{=} \frac{\alpha-(1-p)P_f^b}{p}$, $P_f^b = 0$. Since point $b = (P_f^b, P_d^b)$ is on *ROC curve B*, when $P_f^b = 0$, $P_d^b = 0$. Therefore, $B' = (0,0) = \omega_1^B \in \Omega^B$

Case (2): $s < 0$ when $P_f^a = max(0, \frac{\alpha+p-1}{p})$ and when $P_f^a = min(1, \frac{\alpha}{p})$. In this case, P_d^c is a non-increasing function of P_f^a and the maximum value of P_d^c is achieved at $P_f^a = max(0, \frac{\alpha+p-1}{p})$. If $P_f^a = max(0, \frac{\alpha+p-1}{p}) = 0$, we have $A' = (0,0) = \omega_1^A \in \Omega^A$. If $P_f^a = max(0, \frac{\alpha+p-1}{p}) = \frac{\alpha+p-1}{p} = \frac{\alpha-(1-p)1}{p} = \frac{\alpha-(1-p)P_f^{\omega_{mB}^B}}{p} \overset{\text{from }(C-3)}{=} \frac{\alpha-(1-p)P_f^b}{p}$, $P_f^b = 1$. We have $B' = (1,1) = \omega_{mB}^B \in \Omega^B$.

Case (3): $s \geq 0$ when $P_f^a = max(0, \frac{\alpha+p-1}{p})$ and $s < 0$ when $P_f^a = min(1, \frac{\alpha}{p})$. In this case, when P_f^a increases from $max(0, \frac{\alpha+p-1}{p})$ to $min(1, \frac{\alpha}{p})$, P_d^c is first a non-decreasing function and then a non-increasing function of P_f^a. We define the intersection of two line segments on a piecewise-linear ROC curve as a *corner point* of that ROC curve. The maximum value of P_d^c is achieved at a *corner point* on the graph of P_d^c where the slope of the left line segment at that *corner point* and the slope of the right line segment at that *corner point* have different sign (the sign of s changes at that *corner point*).

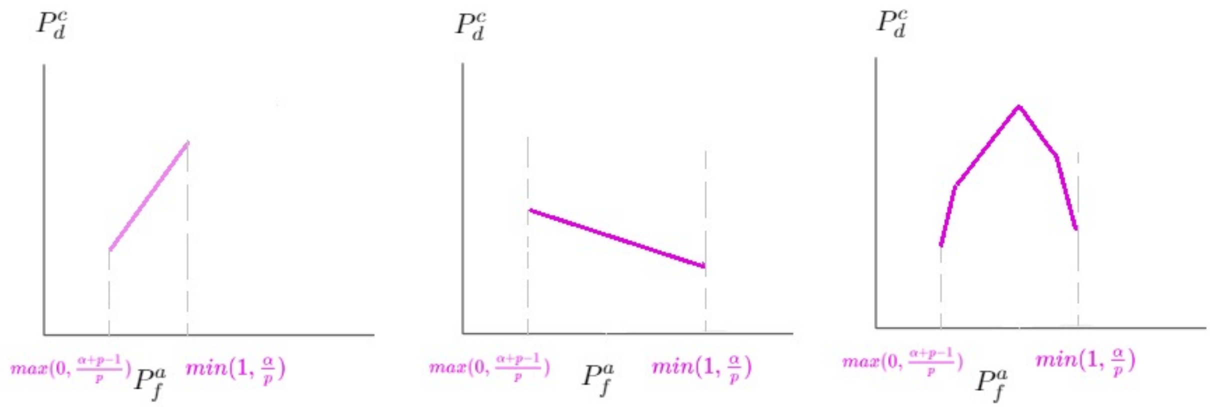

Figure C-2: A graphical illustration of cases (1), (2), and (3) (from left to right).

In cases (1) and (2), P_d^c is a monotonic function of P_f^a, its maximum is achieved when one of the points a and b is at $(0,0)$ or $(1,1)$. Since $\omega_1^A = \omega_1^B = (0,0)$ and $\omega_{mA}^A = \omega_{mA}^B = (1,1)$, either $A' \in \Omega^A$ or $B' \in \Omega^B$ (or both). In case (3), P_d^c is maximized when the sign of s changes from positive to negative. In the expression of s, $p \in (0,1)$, $f_A(.)$ changes only when a is a *corner point* of *ROC curve A* ($A' \in \{\omega_2^A \dots \omega_{mA-1}^A\} \subset \Omega^A$), $f_B(.)$ changes only when b is a *corner point* of *ROC curve B* ($B' \in \{\omega_2^B \dots \omega_{mB-1}^B\} \subset \Omega^B$). Therefore, $P_d^{C'}$ is the maximum probability of detection when either (i) $A' \in \Omega^A$ or (ii) $B' \in \Omega^B$ or both ($A' \in \Omega^A$ and $B' \in \Omega^B$).

C-2. Finding A' from Ω^A if $A' \in \Omega^A$ and B' from Ω^B if $B' \in \Omega^B$ (improved version)

In Section V of the paper, we proposed a 2-step procedure to find A' and B': Step 1 - Finding A' from Ω^A if $A' \in \Omega^A$ and B' from Ω^B if $B' \in \Omega^B$ (Section V-D); Step 2 - Finding A' if $A' \notin \Omega^A$ and B' if $B' \notin \Omega^B$ (Section V-E). Step 1 requires examining all the points in Ω^A and Ω^B ($mA + mB$ points). In this section, we propose a more efficient way to realize Step 1.

In the previous section, we discussed three different cases about finding the maximum of P_d^c, $P_d^{C'}$. We need to first calculate the value of s in (C-6) when $P_f^a = max(0, \frac{\alpha+p-1}{p})$ and when $P_f^a = min(1, \frac{\alpha}{p})$ to determine which case we are encountering.

1) Case (1): P_d^c is a non-decreasing function of P_f^a and the maximum of P_d^c achieved when $P_f^a = min(1, \frac{\alpha}{p})$, shown as the first graph in Figure C-2. When $P_d^{C'}$ is the maximum of probability of detection, we can find either $A' = (P_f^{A'}, P_d^{A'}) = (1, 1)$ or $B' = (P_f^{B'}, P_d^{B'}) = (0, 0)$ (or both).

2) Case (2): P_d^c is non-increasing function of P_f^a and the maximum of P_d^c is achieved at $P_f^a = max(0, \frac{\alpha+p-1}{p})$, shown as the second graph in Figure C-2. When $P_d^{C'}$ is the maximum of probability of detection, we can find either $A' = (P_f^{A'}, P_d^{A'}) = (0, 0)$ or $B' = (P_f^{B'}, P_d^{B'}) = (1, 1)$ (or both).

3) Case (3): P_d^c is first a non-decreasing function and then a non-increasing function of P_f^a. The slope of each line segment of P_d^c is $s = p[f_A(P_f^a) - f_B(P_f^b)]$ (from (C-6)). Our target is to find $a = A' \in \Omega^A$ or $b = B' \in \Omega^B$ such that the sign of $f_A(P_f^a) - f_B(P_f^b)$ changes from positive to negative.

Let $F^A = \{P_f^{\omega_1^A}, .., P_f^{\omega_{mA}^A}\}$ be the probabilities of false alarm of the operating points in $\Omega^A = \{\omega_1^A \dots \omega_1^{mA}\}$. $A' \in \Omega^A$ when $P_f^{A'} \in F^A$.

Let $F^B = \{P_f^{\omega_1^B}, .., P_f^{\omega_{mB}^B}\}$ be the probabilities of false alarm of the operating points in $\Omega^B = \{\omega_1^B \dots \omega_1^{mB}\}$. $B' \in \Omega^B$ when $P_f^{B'} \in F^B$.

In order to meet the probability of false alarm constraint α, from (C-4), when $P_f^{B'} \in F^B =$

$\{P_f^{\omega_1^B},..,P_f^{\omega_{mB}^B}\}$, the probability of false alarm of point A' satisfies $P_f^{A'} \in G^A = \{\frac{\alpha+(p-1)P_f^{\omega_1^B}}{p},\dots\frac{\alpha+(p-1)P_f^{\omega_{mB}^B}}{p}\}$.

Let $H = F^A \bigcup G^A$, when $A' \in \Omega^A$ or $B' \in \Omega^B$ (or both), $P_f^{A'} \in H$. Therefore, our target now is to find $P_f^{A'} \in H$ such that the sign of $f_A(P_f^a) - f_B(P_f^b)$ changes from positive to negative at $P_f^a = P_f^{A'} \in H$.

Recall that $f_a(P_f^a)$ represents the slopes of all straight line segments $w_1^A w_2^A, w_2^A w_3^A, \dots, w_{mA-1}^A w_{mA}^A$ composing *ROC curve A*. $f_a(P_f^a)$ can be expressed as a decreasing piecewise-constant function of P_f^a:

$$f_A(P_f^a) = \begin{cases} \dfrac{P_d^{\omega_{j+1}^A} - P_d^{\omega_j^A}}{P_f^{\omega_{j+1}^A} - P_f^{\omega_j^A}}, P_f^a \in [P_f^{\omega_j^A}, P_f^{\omega_{j+1}^A}), j = 1,\dots,m_A - 1 \\ \dfrac{P_d^{\omega_{m_A}^A} - P_d^{\omega_{m_A-1}^A}}{P_f^{\omega_{m_A}^A} - P_f^{\omega_{m_A-1}^A}}, P_f^a = P_f^{\omega_{m_A}^A} \end{cases}. \tag{C-7}$$

Similarly, $f_b(P_f^b)$ represents the slopes of all straight line segments $w_1^B w_2^B, w_2^B w_3^B, \dots, w_{mB-1}^B w_{mB}^B$ composing *ROC curve B*. $f_b(P_f^b)$ can be expressed as a decreasing piecewise-constant function of P_f^b:

$$f_B(P_f^b) = \begin{cases} \dfrac{P_d^{\omega_{j+1}^B} - P_d^{\omega_j^B}}{P_f^{\omega_{j+1}^B} - P_f^{\omega_j^B}}, P_f^b \in (P_f^{\omega_j^B}, P_f^{\omega_{j+1}^B}], j = 1,\dots,m_B - 1 \\ \dfrac{P_d^{\omega_2^B} - P_d^{\omega_1^B}}{P_f^{\omega_2^B} - P_f^{\omega_1^B}}, P_f^b = P_f^{\omega_1^B} \end{cases}. \tag{C-8}$$

From (C-4), when the probability of false alarm constraint is met $P_f^c = \alpha$, $P_f^b = \frac{\alpha - pP_f^a}{1-p}$. We can rewrite $f_B(P_f^b) = f_B(\frac{\alpha - pP_f^a}{1-p}) = g_A(P_f^a)$ as a function of P_f^a. From (C-3), $P_f^a = \frac{\alpha-(1-p)P_f^b}{p}$. When $P_f^b \in (P_f^{\omega_j^B}, P_f^{\omega_{j+1}^B}]$, $P_f^a \in [\frac{\alpha+(p-1)P_f^{\omega_{j+1}^B}}{p}, \frac{\alpha+(p-1)P_f^{\omega_j^B}}{p})$. $g_A(.)$ can be expressed as:

$$g_A(P_f^a) = f_B(\frac{\alpha - pP_f^a}{1-p}) = \begin{cases} \dfrac{P_d^{\omega_{j+1}^B} - P_d^{\omega_j^B}}{P_f^{\omega_{j+1}^B} - P_f^{\omega_j^B}}, P_f^a \in [\dfrac{\alpha + (p-1)P_f^{\omega_{j+1}^B}}{p}, \dfrac{\alpha + (p-1)P_f^{\omega_j^B}}{p}), j = m_B - 1,\dots,1 \\ \dfrac{P_d^{\omega_2^B} - P_d^{\omega_1^B}}{P_f^{\omega_2^B} - P_f^{\omega_1^B}}, P_f^a = \dfrac{\alpha + (p-1)P_f^{\omega_1^B}}{p} \end{cases}. \tag{C-9}$$

$g_A(P_f^a)$ calculates the slope of the line segment on *ROC curve B* intersecting the vertical line $P_f = P_f^b = \frac{\alpha - pP_f^a}{1-p}$ (the line segment on *ROC curve B* passing through point $b = (P_f^b = \frac{\alpha - pP_f^a}{1-p}, P_d^b)$). $g_A(P_f^a)$ is a piecewise increasing constant function of P_f^a.

Therefore, in case (3), our target becomes finding $P_f^{A'} \in H$ such that the sign of $f_A(P_f^a) - g_A(P_f^a)$ changes from positive to negative at $P_f^a = P_f^{A'}$.

$f_A(P_f^a) - g_A(P_f^a)$ is a piecewise decreasing constant function of P_f^a and its value only changes when $P_f^{A'} \in H$. Since we defined each one of the constant functions composing $f_A(P_f^a) - g_A(P_f^a)$ on a left-closed right-open interval, when $f_A(P_f^a) - g_A(P_f^a)$ changes from positive to negative, $P_f^{A'}$ can be found as the smallest value of P_f^a in H such that $f_A(P_f^a) - g_A(P_f^a) < 0$.

One way to find $P_f^a = P_f^{A'} \in H$ is using a common binary search algorithm which contains following steps:

1) Sort the elements in H
2) Calculate $f_A(P_f^a) - g_A(P_f^a)$ for the middle element in H

   (if H has an even number of elements, use the smaller one of the middle two elements)
3) If the result is negative: eliminate the latter half of H (excluding the middle element);

   Otherwise: eliminate the former half of H (including the middle element)
4) Repeat steps 2) and 3) until H has only one element, which is $P_f^{A'}$

Since $H = F^A \bigcup G^A$ contains at most $mA+mB$ elements (mA elements in F^A and mB elements in G^A), the binary search algorithm performs at most $log(mA+mB)$ iterations.

When $P_f^{A'}$ is found, if $P_f^{A'} \in F^A$, we can use $P_f^{A'}$ to find A' in Ω^A; if $P_f^{A'} \in G^A$, we can calculate $P_f^{B'} = \frac{\alpha - pP_f^{A'}}{1-p}$ (from (C-4)) and use $P_f^{B'}$ to find B' in Ω^B.

After finding A' if $A' \in \Omega^A$ and B' if $B' \in \Omega^B$, we can use Step 2 in Section V-E of the paper to find A' if $A' \notin \Omega^A$ and B' if $B' \notin \Omega^B$.

REFERENCES

[1] I. Y. Hoballah and P. K. Varshney, “Distributed Bayesian signal detection,” *IEEE Transactions on Information Theory*, vol. 35, no. 5, pp. 995–1000, 1989.

[2] S. Thomopoulos, R. Viswanathan, and D. Bougoulias, “Optimal distributed decision fusion,” *IEEE Transactions on Aerospace and Alectronic Aystems*, vol. 25, no. 5, pp. 761–765, 1989.

[3] Y. I. Han, “Randomized fusion rules can be optimal in distributed Neyman-Pearson detectors,” *IEEE Transactions on Information Theory*, vol. 43, no. 4, pp. 1281–1288, 1997.

[4] J. N. Tsitsiklis *et al.*, “Decentralized detection,” *Advances in Statistical Signal Processing*, vol. 2, no. 2, pp. 297–344, 1993.

[5] A. T. Zijlstra, *Calculating the 8th Dedekind Number*. PhD thesis, University of Groningen, 2013.

[6] M. Kam, W. Chang, and Q. Zhu, “Hardware complexity of binary distributed detection systems with isolated local Bayesian detectors,” *IEEE Transactions on Systems, Man and Cybernetics*, vol. 21, no. 3, pp. 565–571, 1991.

[7] S. Acharya, J. Wang, and M. Kam, “Distributed decision fusion using the Neyman-Pearson criterion,” in *17th International Conference on Information Fusion (FUSION)*, pp. 1–7, IEEE, 2014.

[8] P. Willett and D. Warren, “The suboptimality of randomized tests in distributed and quantized detection systems,” *IEEE Transactions on Information Theory*, vol. 38, no. 2, pp. 355–361, 1992.

[9] W. Dong and M. Kam, “Detection performance vs. complexity in parallel decentralized bayesian decision fusion,” in *51st Annual Conference on Information Sciences and Systems, CISS 2017, Baltimore, MD, USA, March 22-24, 2017*, pp. 1–6, 2017.

[10] J. D. Papastavrou and M. Athans, “The team roc curve in a binary hypothesis testing

environment," *IEEE transactions on aerospace and electronic systems*, vol. 31, no. 1, pp. 96–105, 1995.

[11] Q. Yan and R. S. Blum, "On some unresolved issues in finding optimum distributed detection schemes," *IEEE Transactions on signal processing*, vol. 48, no. 12, pp. 3280–3288, 2000.